

Dynamics of a quantum spin liquid beyond integrability – the Kitaev-Heisenberg- Γ model in an augmented parton mean-field theory

Johannes Knolle,¹ Subhro Bhattacharjee,² and Roderich Moessner³

¹*Blackett Laboratory, Imperial College London, London SW7 2AZ, United Kingdom*

²*International Centre for Theoretical Sciences, Tata Institute of Fundamental Research, Bengaluru 560089, India*

³*Max-Planck-Institut für Physik komplexer Systeme, Nothnitzer Str. 38, 01187 Dresden, Germany*

(Dated: January 12, 2018)

We present an augmented parton mean-field theory which (i) reproduces the *exact* ground state, spectrum, and dynamics of the quantum spin liquid phase of Kitaev’s honeycomb model; and (ii) is amenable to the inclusion of integrability breaking terms, allowing a perturbation theory from a controlled starting point. Thus, we exemplarily study dynamical spin correlations of the honeycomb Kitaev quantum spin liquid within the $K - J - \Gamma$ model which includes Heisenberg and symmetric-anisotropic (pseudo-dipolar) interactions. This allows us to trace changes of the correlations in the regime of slowly moving fluxes, where the theory captures the dominant deviations when integrability is lost. These include an asymmetric shift together with a broadening of the dominant peak in the response as a function of frequency; the generation of further-neighbour correlations and their structure in real- and spin-space; and a resulting loss of an approximate rotational symmetry of the structure factor in reciprocal space. We discuss the limitations of this approach, and also view the neutron scattering experiments on the putative proximate quantum spin liquid material, α - RuCl_3 , in the light of the results from this extended parton theory.

I. INTRODUCTION

The ground states of systems with long-ranged entanglement and topological order are notoriously featureless to conventional (local) experimental probes, a fact which greatly complicates their experimental discovery. At the same time, their fractionalised excitations can be much more characteristic and at the same time accessible to regular experiments like inelastic neutron scattering¹ (INS), so that they form a natural target in the search for new and exotic states of matter. Such excitations can be thermally excited at finite temperature, but they are also visible even at zero temperature by considering *dynamical* correlations in the ground state.

The task of calculating such correlators, however, can be quite complicated: while the topological states themselves are usually not easy to describe, capturing their excitations adds another layer of computational complexity as they are highly non-trivial and non-local collective modes in terms of the microscopic degrees of freedom. The way out is often either an exact numerical study on finite-size systems, or the use of approximation schemes whose controllability may be somewhat intransparent.

Against this background, the existence of exactly soluble models has played an important role. While these are few and far between, they have allowed the development of an understanding on a level of detail not available otherwise. This in turn leads to the natural question which aspects of their behaviour are generic, and which are owed to their exact solubility.

The work reported here picks up several strands of this ensemble of questions in the context of the physics of quantum spin liquids (QSL) which serve as examples of long-ranged entangled phases of condensed matter, with many experimentally relevant candidate materials^{2–6}. Our starting point is the Kitaev honeycomb

spin⁷ model with its well-established Z_2 quantum spin liquid phase, in which spins fractionalise, giving way to new degrees of freedom in the form of emergent Majorana Fermions and Z_2 gauge fluxes⁷. Integrability obtains thanks to the non-dynamical nature of the latter giving rise to a block-diagonal form of the Hamiltonian, with each block soluble as a quadratic fermion hopping problem.

This fractionalisation can be captured in a theory of a kind commonly encountered in parton constructions of strongly correlated electron systems in which the spins are written in terms of multiple fractionalised fermionic and/or bosonic partons which then are expected to capture the nature of the low energy theory.^{3,8–18} Such low energy fractionalised excitations transform under projective representations of symmetries of the system^{3,13,19}. Mean field theories (MFTs) of such parton descriptions can then be used to calculate various experimentally relevant quantities such as the dynamic spin structure factor^{20–23}—regularly measured in neutron scattering experiments.

Indeed, various aspects of the of the Kitaev model have been understood in this framework^{24–26}. However, only ground state properties are exactly reproduced but excited states involving multiple flux excitations are only approximate. The underlying reason is that the commonly applied static mean-field approximation removes all dynamic feedback between the different types of emergent fractionalized excitations. For example, flux-flux interactions of the Kitaev QSL mediated via the Majorana Fermions are neglected. Thus, such static parton MFTs give strikingly wrong results, even qualitatively, for the dynamic spin structure factor for the Kitaev model (see below).

Our first main result is to extend this parton framework to capture the exact solution of the full excita-

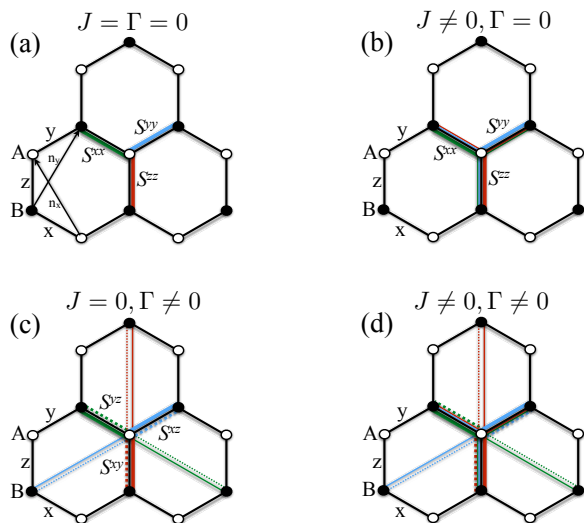


FIG. 1. (Color online) The static correlations of the Kitaev-Heisenberg- Γ model. Colours denote spin components and line thickness schematically the strength of correlations. In the pure Kitaev model, panel (a), these are ultra-short ranged and bond-selective, e.g. along a nearest neighbour bond $\langle ij \rangle_\alpha$ only correlations $S^{\alpha\beta} = \langle S_i^\alpha S_j^\beta \rangle$ with $\alpha = \beta$ are nonzero and all longer range correlations vanish. With weak Heisenberg interactions, panel (b), the bond selectivity is relaxed but spin correlator remain spin-diagonal and exponentially decaying with distance. A Γ perturbation leads exponentially decaying correlations but also to spin-off-diagonal components, panel (c). Both Heisenberg and Γ terms lead to a combination of either correlations. In our treatment correlations are still decaying exponentially with distance and neglecting the algebraically decaying tail is justified by its vanishingly small pre-factor from fourth order perturbation theory²⁷.

tion spectrum at the integrable Kitaev point which requires a more elaborate set-up than the previous static approaches which retains a dynamic feedback between the two types of excitations²².

The Kitaev spin liquid ground state is expected to be perturbatively stable away from the pure Kitaev model because short-ranged four-femion perturbations, which arise from generic bi-linear interaction like Heisenberg exchange, are marginally irrelevant in the renormalisation group sense at the free Majorana fixed point^{24,26}. These expectations are borne out in recent numerical calculations²⁸⁻³¹ which indicate a smooth evolution of the spin dynamics from the Kitaev point throughout the entire QSL phase. These results serve as the motivation to study perturbations, which break the integrability of the starting model, within an augmented dynamical parton MFT set-up.

The second important result of our work is hence to work out the effect of the removal of the fine-tuned static nature of the Z_2 fluxes responsible for integrability, which manifests itself in the reappearance of matrix elements/scattering processes which are absent in the pure Kitaev model. Here, we provide a detailed study of

the changes to the dynamical structure factor, the main ingredient of which is the addition of dynamics to the gapped flux degrees of freedom. This we cannot treat exactly, but instead consider them as a slow variable in a heavy flux approximation, which presents a heuristically motivated first pass at the problem as long as the fluxes remain gapped and their bandwidth continues to be small compared to the bare energy scale of the magnetic exchange.

The dynamical structure factor of the pure Kitaev model is dominated by a narrow peak carrying most of the total spectral weight above a small gap^{32,33}. In agreement with prior work²⁷, we find that the gap is filled in beyond the static flux limit. The most visible consequence of the integrability-breaking terms is an asymmetric broadening of the peak in frequency of the dynamical response on a scale set by the perturbation. In addition, a qualitative change is that previously vanishing correlators acquire non-zero values, which applies both to correlators between different spin components, and to correlators between spatially separated spins; however, the latter do not do so uniformly but rather retain memory of the two-sublattice structure of the honeycomb lattice²⁷.

In third step, we also discuss limitations of our approach, which fundamentally arise from its neglect of multiple-scattering processes between the Majoranas and the fluxes, which among other things are ultimately responsible for recombining the fractionalised degrees of freedom en route to a magnetic ordering transition out of the spin liquid.

Our final set of results is a contribution to the current discussion on the relation of the Kitaev model to the physics of the magnetic material α -RuCl₃, which has been billed a proximate spin liquid on account of its unusual high-energy/finite-temperature dynamical response³⁴⁻³⁸, for recent reviews see Ref. 39 and 40. We show that some of the discrepancies between the exact solution of the Kitaev spin liquid and the experimental results are remedied as perturbations are added. For example the hexagonal star-like features of the neutron scattering response appears naturally in this treatment and the spectral weight is less concentrated in a single narrow low energy peak.

The remainder of this paper is structured as follows. Sec. II starts with the definition of the model and introduces notation. Sec. III contains the development of the dynamical mean-field theory for the partons, with some technical content relegated to an appendix, which the reader not primarily interested in those technical developments may want to skip upon first reading. Sec. IV contains a detailed discussion of the properties of the dynamical structure factor summarised above, as the central observable of interest in spectroscopic experiments such as neutron scattering experiments. Its last subsection is devoted to a discussion of the experimental situation in α -RuCl₃ in the light of our present theory. We close with a discussion and an outlook in Sec. V.

II. THE SPIN SYSTEM AND THE DYNAMIC SPIN STRUCTURE FACTOR

Our objective is to study the evolution of the dynamical spin correlations in the Kitaev QSL phase when perturbed from the exactly solvable point. Experimentally, in candidate spin liquid materials, the most interesting set of perturbations to the Kitaev model involve the usual Heisenberg perturbations, and the pseudo-dipolar perturbations. Hence we wish to understand the nature of spin correlations in presence of such perturbations. Thus, our starting point is the so called Kitaev-Heisenberg- Γ (KHF) model given by the Hamiltonian

$$H = \sum_{\langle ij \rangle_\alpha} \left\{ K S_i^\alpha S_j^\alpha + J \sum_\beta S_i^\beta S_j^\beta + \Gamma \sum_{\beta \neq \beta \neq \alpha} S_i^\beta S_j^\beta \right\} \quad (1)$$

with spin components $\alpha, \beta = x, y, z$ which also label the three inequivalent bond directions $\langle ij \rangle_\alpha$ on the honeycomb lattice, see Fig.1 (a). $S_i^\alpha = \sigma_i^\alpha / 2$ are the spin-1/2 operators with σ_i^α being the Pauli matrices ($\alpha = x, y, z$). We concentrate on isotropic couplings throughout and measure all energies in units of $|K|$. As our work is partially motivated by experimental results on α -RuCl₃ we follow the emerging consensus³¹ that the leading interaction is a FM Kitaev term, e.g. for concreteness we set $K = -1$ (FM couplings) and mainly concentrate on FM $J \leq 0$ and AFM $\Gamma \geq 0$.

The dynamic spin structure factor,

$$S^{\alpha\beta}(\mathbf{q}, \omega) = \frac{1}{N} \sum_{ij} e^{i\mathbf{q} \cdot (\mathbf{r}_i - \mathbf{r}_j)} \int dt dt' e^{-i\omega(t-t')} \langle S_{\mathbf{r}_i}^\alpha(t) S_{\mathbf{r}_j}^\beta(t') \rangle, \quad (2)$$

experimentally measured through neutron scattering for magnetic insulators yields direct information about the nature of spin-spin correlations present in the system and hence can shed light on the nature of the ground state of the spin system. For the pure Kitaev model the dynamic structure factor can be exactly calculated as the Z_2 fluxes are immobile^{32,33,41,42} which leads to distinct signatures arising from the strictly non-dispersive gapped Z_2 fluxes and gapless Majorana fermions. A central ingredient in the exact calculation is the non-dispersive nature of the flux which then was used to map the calculations into one of a quenched impurity to obtain the exact solutions. In contrast to the previous work^{32,33} we wish to go beyond the integrable point which then has to incorporate the central issue of dispersing Z_2 fluxes, which in turn maps to a problem of a quenched *dynamical* impurity. Given the notorious difficulties of time dependent perturbation theory, particularly with fluxes with gauge strings, we will exploit a different route via an extension of parton MFTs taking into account fluctuations of the emergent Z_2 gauge field.

III. PARTON THEORY FOR THE HKT MODEL

Any parton description of the perturbed Kitaev spin liquid must incorporate the exact solution as a quantitatively well defined limiting case where: (a) the Z_2 flux excitations are gapped with the right magnitude of the two flux gap, (b) spin-correlations are exactly nearest neighbour, and (c) the correct excitation spectrum which then produces the right distribution of spectral weights in the dynamic spin structure factor for example. These features then carry on in the perturbative regime with some modifications such as the spin-correlations become exponentially decaying⁴³ [up to a small algebraic contribution²⁷ if both $J \neq 0$ and $\Gamma \neq 0$ at fourth order $O(J^2\Gamma^2)$]. A characteristic feature of this perturbative regime is a natural separation of scale emerges between the 'fast' itinerant Majorana fermions and the 'slow' gapped flux excitations which will allow us to use a 'heavy flux' approximation to the flux dynamics as detailed below.

Previous works have shown that simple parton MFTs of the Kitaev model recover some of the exact ground state properties^{24,26} which is based on the fact that spins 'exactly' fractionalize into itinerant Majorana fermions and Z_2 fluxes⁴⁴, and the emergent Z_2 gauge field is static at the exactly solvable point. Hence the fluxes can be thought of as a classical background field for the Majorana fermions.

However, these simple MFTs fail to correctly capture the full physics of the Kitaev model even at the integrable point. In particular, the description of excited states involving flux excitations is wrong because any feedback between fluxes and fermions is neglected within these MFT approaches where the mean field parameters are static and hence lead to wrong matrix elements arising from the zero flux sector which are absent in the exact calculations because the corresponding matrix elements are zero. Here we augment the MFT with fluctuations which are then used to calculate the correct dynamical response of the spins.

We follow the original work of Kitaev⁷ and use a representation of the spin operator in terms of four Majorana fermions

$$S_i^\alpha = \frac{1}{2} i c_i b_i^\alpha. \quad (3)$$

with $\{b_i^\alpha, b_j^\beta\} = 2\delta_{ij}\delta_{\alpha\beta}$ (similarly for c_i). The key ingredient for the solubility of the pure Kitaev model, $J = \Gamma = 0$, is the presence of an extensive number of local conserved quantities (with eigenvalues ± 1)

$$W_p = \prod_{i \in \partial_p} 2S_i^\beta = \prod_{\langle ij \rangle_\alpha \in \partial_p} i b_i^\alpha b_j^\alpha \delta_{\langle ij \rangle_\alpha}. \quad (4)$$

The product includes all spin operators of a hexagon and there spin component β is given by the outward pointing bond type. These plaquette fluxes permit a block-diagonalization of the Hamiltonian and the overcomplete representation of the spin Hilbert space in terms

of the Majorana fermion operators entails a Z_2 gauge redundancy^{45–47}.

It is convenient to split the Hamiltonian, Eq.1, into Kitaev- and non-Kitaev contributions

$$H = -\frac{K+J}{4} \sum_{\langle ij \rangle_\alpha} (ib_i^\alpha b_j^\alpha) ic_i c_j - \frac{J}{4} \sum_{\langle ij \rangle_\alpha} \sum_{\beta \neq \alpha} (ib_i^\beta b_j^\beta) ic_i c_j - \frac{\Gamma}{4} \sum_{\langle ij \rangle_\alpha} \sum_{\beta \neq \alpha} (ib_i^\beta b_j^{\bar{\beta}}) ic_i c_j. \quad (5)$$

Explicitly, the combination of spin operators in the last term is for example along an $\alpha = z$ bond: $\{\beta, \bar{\beta}\} = \{x, y\}, \{y, x\}$.

The presence of the J and Γ term renders the model unsolvable by making the Z_2 fluxes dynamic, i.e., in presence of J and Γ , the W_p s no longer commute with the Hamiltonian. However, it is very important to ask both from the theoretical side as well as in regards to possible experimental candidates – what features of the fractionalised excitations, as encoded in the dynamic structure factor survive in presence of such perturbation?

To answer this question, in absence of the exact solution, a natural candidate is an appropriate parton MFT which can then be utilised to calculate the dynamic spin structure factor.

A. Static parton MFT for the ground state of the Kitaev model

The presence of the formal exact solution for the Kitaev model raises the question of testing the validity, in context of the pure Kitaev model, of mean-field approaches to the fractionalised phases within the ambit of the parton MFTs which have been developed over the years to understand the qualitative features of these phases.^{3,8–18}

Within such formulation, which naturally gives rise to low energy effective lattice gauge theories with dynamic matter and gauge fields, it is found that the Kitaev ground state is reproduced with some control as the gauge fields become frozen at the exactly solvable point. While several formulations exist^{24,26}, we focus on the Majorana mean field formalism which we shall use for the rest of this work²⁵. Within this formalism, the Hamiltonian in Eq.5 is decoupled using the following mean-field channels:

$$\langle ic_i c_j \rangle = \chi^c \quad (6)$$

$$\langle ib_i^\alpha b_j^\alpha \rangle = \chi_K^b \quad (7)$$

$$\langle ib_i^\beta b_j^\beta \rangle = \chi_J^b \text{ with } \beta \neq \alpha \quad (8)$$

$$\langle ib_i^\beta b_j^{\bar{\beta}} \rangle = \chi_\Gamma^b \text{ with } \bar{\beta} \neq \beta \neq \alpha \quad (9)$$

which captures the Kitaev ground state – a single linearly dispersing Majorana fermion (c) and three gapped non-dispersing Majorana fermions (b^α s) with the flat-band of

the latter being related to the conservation of Z_2 fluxes of the exact solution.

The strength of the above MFT becomes evident when one considers finite perturbations $J, \Gamma \neq 0$ to the pure Kitaev model as denoted by Eq.5. While the exact solution is no longer available, the parton MFT can be used to qualitatively understand the effect of the perturbation on the spin liquid ground state and even the transition to a proximate magnetically ordered state as in Ref.26.

However, while the above MFT does faithfully capture the ground state, it fails to account for the spin-spin correlations because within the simple decoupling the spin-spin correlations are given by

$$\langle S_i^\alpha(t) \sigma_j^\beta(0) \rangle \sim \langle ib_{i,t}^\alpha b_{j,0}^\beta \rangle \langle ic_{i,t} c_{j,0} \rangle$$

which yields both qualitatively and quantitatively the wrong spin structure factor as it misses the crucial matrix element effects which mixing different Z_2 flux sectors^{32,33,44}.

The lacunae of this static parton MFT need to be rectified to gain control over the calculation of the dynamic structure factor. To this end, we present an augmented parton theory which contains the minimal feedback, as explained below, to reproduce the exact dynamic structure factor at the exactly solvable point which then forms the basis of its systematic calculations in presence of small perturbations.

B. Augmented Z_2 parton MFT

We now incorporate the feedback to correct for the dynamics within the parton description by including fluctuations around the mean-field. In addition to the amplitude fluctuations $\hat{\delta}^{\alpha/c}$ we also include the ones of the overall sign $\hat{\sigma}_{ij}^\alpha$ corresponding to the Z_2 gauge fluctuations. The eigenvalues of $\hat{\sigma}_{ij}^\alpha$ are ± 1 . It is motivated by the exact solution in which the link variables $u_{ij} = ib_i^\alpha b_j^\alpha$ are constants of motion with eigenvalues ± 1 . Hence, we augment the decoupling channels of Eq.6ff as follows. Along an α -type bond $\langle ij \rangle_\alpha$

$$ic_i c_j = \chi^c + \hat{\delta}_{ij}^c \quad (10)$$

$$ib_i^\alpha b_j^\alpha = \hat{\sigma}_{ij}^\alpha (\chi_K^b + \hat{\delta}_{ij,K}^\alpha) \quad (11)$$

$$ib_i^\beta b_j^\beta = \chi_J^b + \hat{\delta}_{ij,J}^\beta \text{ with } \beta \neq \alpha \quad (12)$$

$$ib_i^\beta b_j^{\bar{\beta}} = \chi_\Gamma^b + \hat{\delta}_{ij,\Gamma}^\beta \text{ with } \bar{\beta} \neq \beta \neq \alpha. \quad (13)$$

where we have explicitly put the hat on the fluctuations to point out that they are quantum operators. Of particular importance in the rest of this calculation is the Z_2 link variable with the properties

$$\hat{\sigma}_{ij}^\alpha = -\hat{\sigma}_{ji}^\alpha \text{ and } \{b_i^\alpha, \hat{\sigma}_{ij}^\alpha\} = 0. \quad (14)$$

We note that the flavour $\alpha = x, y, z$ of the bond variable $\hat{\sigma}_{ij}^\alpha$ depends on the type of bond. This allows us to minimally incorporate the flux dynamics via the new Z_2 link

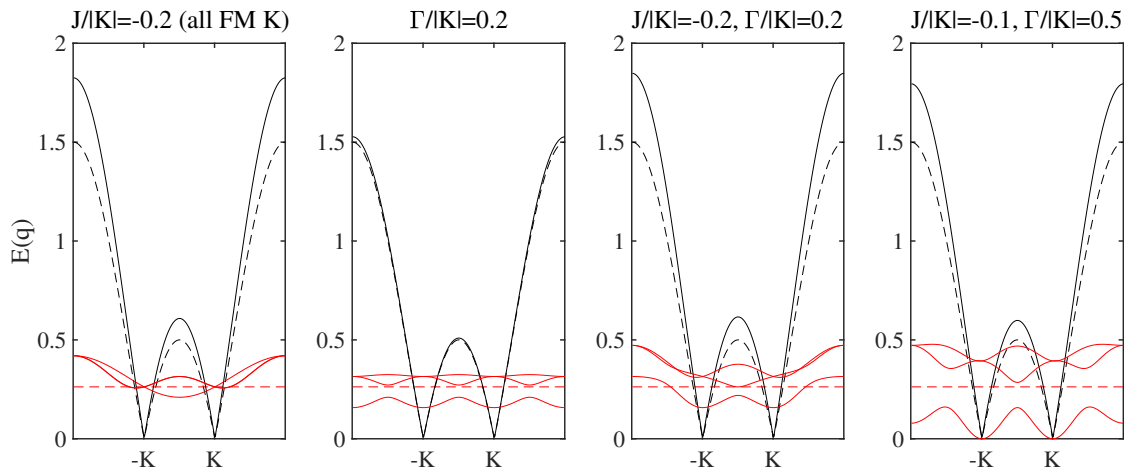


FIG. 2. (Color online) The MFT dispersions of the matter c -type (black) and flux b -type (red) Majorana Fermions for different regimes compared to the exactly soluble point (dashed). The dynamical structure factors for each parameter set are shown below.

variable which corresponds to the the plaquette flux of the pure Kitaev model (where $\chi_K^b = 1$, see below)

$$W_p = \prod_{\langle ij \rangle_\alpha \in \partial_p} i b_i^\alpha b_j^\alpha \delta_{\langle ij \rangle_\alpha} = \prod_{\langle ij \rangle_\alpha \in \partial_p} \hat{\sigma}_{ij}^\alpha. \quad (15)$$

The spin operators flip the W_p 's which is ensured in our augmented Z_2 MFT because we now have the property of the link variables of the exact solution $\{b_i^\alpha, u_{ij}^\alpha\} = 0$. This introduces a direct coupling between the c -type Majorana matter fermions and the b -type flux fermions. It is this ingredient which was missed in previous MFTs and which is crucial for recovering the full exact solution – both statics as well as the dynamics.

In a standard MFT approximation we neglect the quadratic part of the amplitude fluctuations, but keeping the phase fluctuations as represented by $\hat{\sigma}_{ij}^\alpha$ such that the Hamiltonian is bilinear and can be split into matter- and flux-Majorana fermion parts $H_{\text{MFT}} = H^b + H^c + C$ with

$$\begin{aligned} H^c &= -\frac{1}{4} \sum_{\langle ij \rangle_\alpha} \{ \hat{\sigma}_{ij}^\alpha (K+J) \chi_K^b + 2J \chi_J^b + 2\Gamma \chi_\Gamma^b \} i c_i c_j \quad (16) \\ H^b &= -\frac{1}{4} \sum_{\langle ij \rangle_\alpha} \left\{ (K+J) \chi^c i b_i^\alpha b_j^\alpha + J \chi^c \sum_{\beta \neq \alpha} i b_i^\beta b_j^\beta \right\} + \\ &\quad -\frac{1}{4} \sum_{\langle ij \rangle_\alpha} \Gamma \chi^c \sum_{\beta \neq \alpha} i b_i^\beta b_j^\beta \\ C &= \frac{K+J}{4} \chi_K^b \chi^c \sum_{\langle ij \rangle_\alpha} \hat{\sigma}_{ij}^\alpha + \frac{N_b \chi^c}{2} (J \chi_J^b + \Gamma \chi_\Gamma^b) \end{aligned}$$

with N_b the total number of bonds. Note, there is an explicit dependence of the constant C on the configuration of the Z_2 variables.

This then forms the augmented parton theory that contains minimal ingredients required to reproduce the

exact results at the Kitaev point and then can be used to understand the effect of the perturbations on the dynamic spin structure factor.

Having set up the augmented parton Z_2 MFT, the next steps are essentially standard derivations of the mean-field solutions including the enforcement of self-consistency, as detailed in App. A. From this, we display the resulting MFT-dispersions, which demonstrate the (weak) dispersion arising for the previously immobile fluxes, see Fig. 2. Note that we have not allowed for a magnetic ordering instability in this theory, so that the fluxes become gapless (right panel Fig. 2) without triggering a phase transition. We will return to this point in our discussion of α -RuCl₃ below.

At this point, we note that previous parton MFTs investigating the HK model including magnetic decoupling channels found a first order transition from the Kitaev spin liquid to a gapped fractionalised $U(1)$ spin liquid with simultaneous magnetic order²⁶. It was argued there that the fractionalisation is a pathological feature of the mean field theory which undergoes confinement on incorporating instanton effects. Here we do not include the magnetic parameters and hence our calculations are strictly valid only in the vicinity of the pure Kitaev limit.

C. Dynamical Spin Correlations and Mapping to a Quantum Quench

Next we focus on our main objective which is to study the dynamical spin correlation function of the Kitaev QSL

$$S_{ij}^{\alpha\beta}(t) = \langle 0 | S_i^\alpha(t) S_j^\beta(0) | 0 \rangle \quad (17)$$

and we restrict the discussion to zero temperature when $|0\rangle$ denotes the the ground state.

We rewrite the spin operators in terms of Majorana fermions, Eq.3, and concentrate on the inter-sublattice component for concreteness

$$S_{A0B\mathbf{r}}^{\alpha\beta} = -\frac{1}{4}\langle 0|e^{it(H^b+H^c+C)}c_{A0}b_{A0}^\alpha e^{-it(H^b+H^c+C)}c_{B\mathbf{r}}b_{B\mathbf{r}}^\beta|0\rangle. \quad (18)$$

A major advantage in the augmented MFT is the fact that the flux and matter fermions are not directly coupled. Hence, we would like to write the correlator as a simple product of b -type and c -type correlation functions similar to the derivation for the pure Kitaev model as pioneered by Baskaran et al.⁴⁴. However, we have to keep in mind that both types of fermions are indirectly coupled via the Z_2 link variable.

First, we split the exponential via the Baker-Hausdorff formula

$$e^{-it(H^b+H^c)} = e^{-itH^c} e^{-itH^b} e^{\frac{t^2}{2}[H^b, H^c]} \approx e^{-itH^c} e^{-itH^b}.$$

Note, because of our Z_2 variable both terms do not commute, but it is easy to show that $[H^b, H^c] \propto J\chi_j^b \dots + \Gamma\chi_\Gamma^b \dots \propto O(J^2, \Gamma^2)$. Hence, in the limit $J/K, \Gamma/K \ll 1$ (for small t generally) the commutator can be neglected.

Second, we commute the operators past the exponentials. With the commutation properties Eq.14 we obtain

$$b_{A0}^\alpha H^c = \underbrace{[H^c + V_{A0}^\alpha]}_{H^c \text{ with } \sigma_{A0B\mathbf{n}_\alpha}^\alpha \text{ flipped}} b_{A0}^\alpha \quad (19)$$

$$b_{A0}^\alpha C = [C + C_{A0}^\alpha] \text{ with } C_{A0}^\alpha = -\frac{K+J}{2}\chi_K^b \chi^c. \quad (20)$$

It shows that the action of a spin operator introduces a pair of n.n. fluxes which in turn alters the dynamics of the matter fermions^{32,33,48}. Hence, the spin correlation function is mapped to the calculation of a quantum quench. From Eq. 18 we thus get

$$S_{A0B\mathbf{r}}^{\alpha\beta}(t) = \frac{1}{4}e^{iE_0^c t} \times \langle 0|c_{A0}e^{-it(H^c+V_{A0}^\alpha)}e^{-itC_{A0}^\alpha}c_{B\mathbf{r}}e^{itH^b}b_{A0}^\alpha e^{-itH^b}b_{B\mathbf{r}}^\beta|0\rangle. \quad (21)$$

Crucially, the states of the matter sector depend on the flux sector. General states of the MF Hamiltonian take the form $|M\rangle = |M_c\{\sigma\}\rangle|M_b\rangle$ because the occupation of the b -type fermions also determine the link variable $\hat{\sigma}_{ij}^\alpha$. For nonzero J, Γ , fluxes are not static and the flipped flux from Eq.21 can actually disappear. So, stated differently, the position of the impurity potential seen by the c fermions depends on the dispersion of the b fermions which in turn determine $\langle \hat{\sigma}_{ij}^\alpha \rangle = \sigma_{ij}$. Hence we can write the dynamical spin correlations as a product of the form

$$S_{A0B\mathbf{r}}^{\alpha\beta}(t) = \delta_{\alpha\beta} \frac{1}{4}e^{iE_0^c t} \langle 0_c|c_{A0}e^{-it[H^c+V_{A0}^\alpha(\{b\})]}e^{-itC_{A0}^\alpha(\{b\})}c_{B\mathbf{r}}|0_c\rangle \times \langle 0_b|e^{itH^b}b_{A0}^\alpha e^{-itH^b}b_{B\mathbf{r}}^\beta|0_b\rangle. \quad (22)$$

D. The heavy flux approximation

Eq.22 is in itself not straightforward to evaluate in general. In order to make progress, we need to identify a

scheme for evaluating this expression which is tractable near the exactly soluble point. In the following, we explain such a heavy flux approximation which, as we discuss further down, is not systematically controlled but correctly captures several of the central features of the change in the dynamical behaviour as integrability is discarded.

For small J, Γ as long as the flux gap remains large the fluxes are much slower (heavier) than the gapless matter fermions. For example, the mass of the fluxes or the b fermions are order $1/J$ for $\Gamma = 0$, see the red lines in Fig. 2. Looking at the decay time of the flux-Majorana propagator

$$G_{A0B\mathbf{r}}^\alpha(t) = i\langle 0_b|b_{A0}^\alpha(t)b_{B\mathbf{r}}^\alpha|0\rangle \quad (23)$$

at $\mathbf{r} = 0$ we can calculate the average time τ after which a flux pair has disappeared from a given plaquette by hopping away, e.g. from the condition $|G_{A0B0}^\alpha(t)| \leq \frac{1}{2}$. This directly introduces a time dependence for our potential and in the simplest form it is just abruptly switched off once the flux hopped away $V_{A0}^\alpha(t) = V_{A0}^\alpha\Theta(\tau-t)$ (where τ sets the decay time calculated from the above mentioned condition and Θ is the Heavyside function). The decay of the propagator $|G_{A0B0}^\alpha(t)|$ is shown in Fig.3 for various J, Γ . Note, for small J and $\Gamma = 0$ (small Γ and $J = 0$) the decay time scales as $\tau \propto J^{-1}$ ($\tau \propto \Gamma^{-1}$) as expected from the scaling of the mass of the b -fermions.

Finally, with the matter fermion correlator

$$G_{A0B\mathbf{r}}^c(t, \tau) = ie^{iE_0^c t} \langle 0_c|c_{A0}e^{-it[H^c+V_{A0}^\alpha\Theta(\tau-t)]}c_{B\mathbf{r}}|0_c\rangle \quad (24)$$

we obtain an expression which is a simple product of time dependent matter and flux fermion propagators

$$S_{A0B\mathbf{r}}^{\alpha\beta}(t) = -\frac{1}{4}e^{it\Delta_b} G_{A0B\mathbf{r}}^c(t, \tau) G_{A0B\mathbf{r}}^{\alpha\beta}(t), \quad (25)$$

and similarly for $S_{A0A\mathbf{r}}^{\alpha\beta}(t)$ [the explicit definition of $G_{A0B\mathbf{r}}^{\alpha\beta}$ is given below; Note, for $G_{A0A\mathbf{r}}^c(t, \tau)$ just replace $c_{B\mathbf{r}} \rightarrow c_{A\mathbf{r}}$ but the local potential V_{A0}^α is always at site $A0$]. This factorized form of the spin correlation function is the main result of the derivation. Crucially, it allows us to calculate the flux and matter Majorana propagator separately via our augmented Z_2 MFT.

1. Expression for the fermionic propagators

For the matter fermions at times $t < \tau$ it is necessary to evaluate the full local quantum quench including the impurity potential, see Eq. 24. This is done on large real space lattice (65×65 unit cells) using the methods of our previous works^{33,48}. Once the flux has disappeared the calculation is much easier and given by (see App. A for details and definitions)

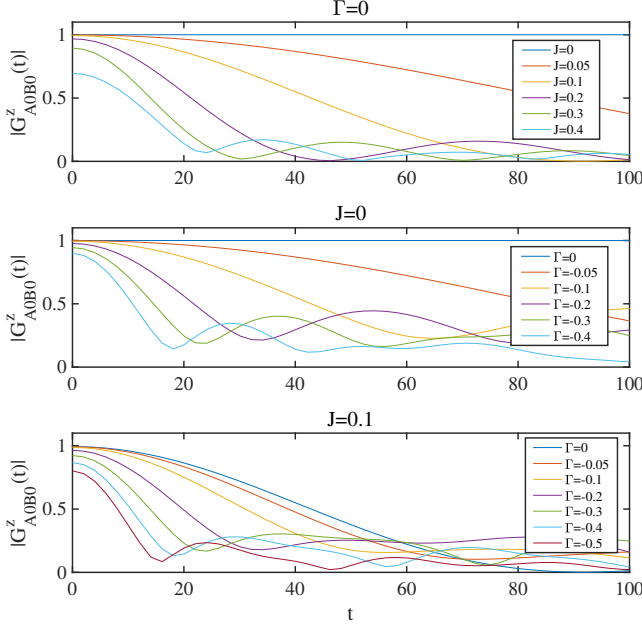


FIG. 3. The decay of the flux propagator $G_{A_0 B_0}^z(t)$ which is related to the time dependence of the Z_2 link variable is shown for various values of J, Γ . The average time τ after which a flux has hopped away can be read off. Note that the suppression of the propagator below unity at $t = 0$ reflects the admixture of fluxes into the ground state, which is flux-free only at the integrable point.

$$G_{A_0 B_{\mathbf{r}}}^c(t > \tau) = i \langle 0_c | c_{A_0}(t) c_{B_{\mathbf{r}}} | 0_c \rangle = \sum_{\mathbf{q}} e^{-it2|S(\mathbf{q})|} \{ e^{i\mathbf{q}\mathbf{r}} \cos^2 \theta_{\mathbf{q}} - e^{-i\mathbf{q}\mathbf{r}} \sin^2 \theta_{\mathbf{q}} - 2 \sin \theta_{\mathbf{q}} \cos \theta_{\mathbf{q}} \sin \mathbf{q}\mathbf{r} \} \quad (26)$$

$$G_{A_0 A_{\mathbf{r}}}^c(t > \tau) = i \langle 0_c | c_{A_0}(t) c_{A_{\mathbf{r}}} | 0_c \rangle = i \sum_{\mathbf{q}} e^{-it2|S(\mathbf{q})|} \{ e^{i\mathbf{q}\mathbf{r}} \cos^2 \theta_{\mathbf{q}} + e^{-i\mathbf{q}\mathbf{r}} \sin^2 \theta_{\mathbf{q}} \}. \quad (27)$$

For a smooth Fourier transformation to frequency space we match up the solutions from $G_{A_0 B_{\mathbf{r}}}^c(t < \tau)$ with $G_{A_0 B_{\mathbf{r}}}^c(t > \tau)$. In practice the propagators are glued together as

$$G_{A_0 B_{\mathbf{r}}}^c(t, \tau) = [1 - f(t, \tau)] G_{A_0 B_{\mathbf{r}}}^c(t, \tau = t) + f(t, \tau) G_{A_0 B_{\mathbf{r}}}^c(t, \tau = 0) \quad (28)$$

with the smoothed out step function $f(t, \tau) = \frac{1}{1 + e^{-t/\tau}}$.

Finally, the flux propagators are calculated from

$$G_{A_0 B_{\mathbf{r}}}^{\alpha\beta}(t) = - \sum_{\mathbf{q}} e^{i(\mathbf{q}\mathbf{r} - t\epsilon_{\mathbf{q}}^j)} U_{j\mathbf{q}}^{\alpha} V_{j\mathbf{q}}^{\beta} \quad (29)$$

$$G_{A_0 A_{\mathbf{r}}}^{\alpha\beta}(t) = -i \sum_{\mathbf{q}} e^{i(\mathbf{q}\mathbf{r} - t\epsilon_{\mathbf{q}}^j)} U_{j\mathbf{q}}^{\alpha} U_{j\mathbf{q}}^{\beta*}. \quad (30)$$

where $U_{j\mathbf{q}}^{\alpha}$ and $V_{j\mathbf{q}}^{\alpha}$ are coherence factors obtained by diagonalising the MFT Hamiltonian as discussed below, see Eq.A11 in the appendix.

E. Recovery of the exact solution

We close this section with the demonstration – in contrast to previous parton MFT treatments^{24,26} – that our augmented MFT (i) recovers the full exact solution including all excited states at the integrable Kitaev point with $J, \Gamma = 0$ (ii) and as such can be used to compute the exact dynamical correlations at this point as well.

As in the exact solution⁴⁴ the static spin correlations in the ground state are only nonzero for on-site and nearest-neighbor correlators

$$S_{A_0 B_{\mathbf{r}}}^{\alpha\beta} = -\frac{1}{4} \langle 0 | c_{A_0} b_{A_0}^{\alpha} c_{B_{\mathbf{r}}} b_{\mathbf{r}}^{\beta} | 0 \rangle \quad (31)$$

$$= \delta_{\mathbf{n}_{\alpha}, \mathbf{r}} \delta_{\beta, \alpha} \chi^c \chi_K^b = -\text{sgn}[K] 0.5249$$

because the dispersion of the b -type flux Majoranas is a flat band²⁶ which also gives $\chi_K^b = 1$.

Excitations of the c -type matter fermions in the ground state flux sector are obviously the same as in the exact

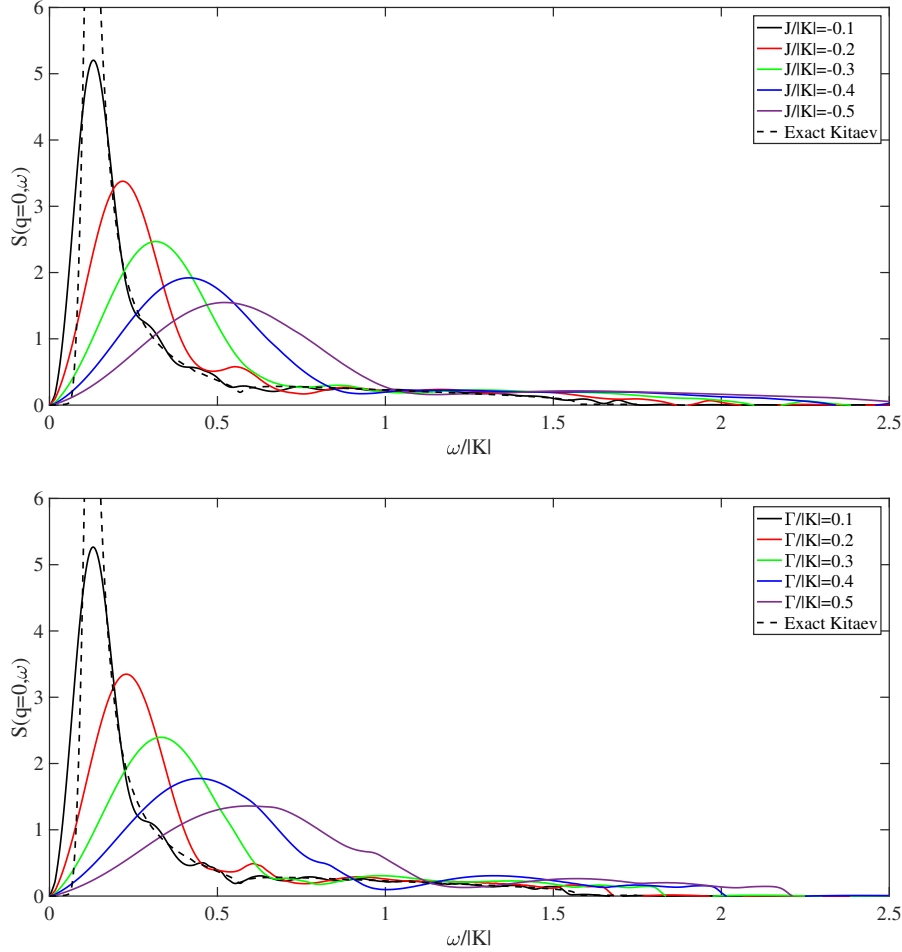


FIG. 4. Evolution of the dominant peak of the structure factor $S(\mathbf{q} = 0, \omega)$ of the FM Kitaev model as a function of perturbing Heisenberg (J) (top) and Γ -interaction (bottom). Note the asymmetric broadening accompanying a shift of the centre on a scale set by the strength of the perturbation.

solution, see Eq.A5. What about the flux excitations? At first sight it seems that pairs of nearest neighbor flux excitations arise from populating the flat b -type bands with energy $E_b = \frac{K\chi^c}{2}$ see Eq.A10. However, this contradicts the exact solution where a flux excitation costs an energy $E_b = \frac{K\chi^c}{8}$. Moreover, exciting N pairs of fluxes is not just N times E_b from populating N flux b-fermions in the flat band. In the exact solution fluxes interact via coupling to the c -type matter Majorana background reducing the overall energy of multiple flux excitations⁷.

Nevertheless, a careful consideration of the definition of the energy of a flux excitation shows that our augmented MFT is nothing but an alternative form of the exact solution in contrast to previous MFTs^{24,26}. The energy of a pair of fluxes is defined as the energy difference

$$E_b = \langle 0 | b_{A0}^z H b_{A0}^z | 0 \rangle - \langle 0 | H | 0 \rangle. \quad (32)$$

Keeping in mind all terms in the MFT Hamiltonian Eq.16 including the constants and the fact that the ground state

of the matter Fermions depends on the flux background $|0\rangle = |0_c \{\sigma\}\rangle |0_b\rangle$ via the link variable σ_{ij}^α (e.g. $|0_c \{+\nabla\}\rangle$ labels the matter g.s. in the flux free sector with all $\sigma_{ij} = +1$) we see that

$$\begin{aligned} \langle 0 | H | 0 \rangle &= \underbrace{\langle \{+\nabla\} 0_c | H_c | 0_c \{+\nabla\} \rangle}_{E_0^c \{+\nabla\} = -\sum_{\mathbf{q}} |S(\mathbf{q})|} + \underbrace{\langle 0_b | H_b | 0_b \rangle}_{E_0^b = -\frac{3K\chi^c N_B}{4}} + \frac{K\chi_K^b \chi^c N_B}{4} \\ &= -\frac{K\chi^c N_B}{2} + E_0^c \{+\nabla\} \end{aligned}$$

and

$$\begin{aligned} \langle 0 | b_{A0}^z H b_{A0}^z | 0 \rangle &= \underbrace{\langle \{\sigma_{A0B0}^z = -1\} 0_c | H_c | 0_c \{\sigma_{A0B0}^z = -1\} \rangle}_{E_0^c \{\sigma_{A0B0}^z = -1\}} + \\ &\quad \underbrace{\langle 0_b | b_{A0}^z H_b b_{A0}^z | 0_b \rangle}_{E_1^b = -\frac{3K\chi^c N_B}{4} + \frac{K\chi^c}{2}} + \frac{K\chi_K^b \chi^c (N_B - 2)}{4} \\ &= -\frac{K\chi^c N_B}{2} + E_0^c \{\sigma_{A0B0}^z = -1\} \end{aligned}$$

such that the flat band contribution is exactly canceled by the constants and we recover the exact energy of a pair of flux excitations which is nothing but the difference in ground state energies of the matter Majoranas with and without a pair of fluxes in the background

$$E_b = E_0^c \{ \sigma_{A_0 B_0}^z = -1 \} - E_0^c \{ +\nabla \}. \quad (33)$$

The same reasoning shows that all excited state energies including multiple fluxes are correct in our description.

It is somewhat surprising that the flat band flux Fermions completely drop out as physical degrees of freedom.

With this in hand, we can also demonstrate that the augmented mean-field theory recovers the exact solution of the dynamical structure factor. Note for $\Gamma = 0$ the Hamiltonian is diagonal in the different types of b^α Majoranas which directly gives $S^{\alpha\beta} \propto \delta_{\alpha,\beta}$. For $J, \Gamma = 0$ the b -type propagator is simply $G_{A_0 B_r}^z(t) = \delta_{r,0} e^{-it \frac{K\chi^c}{2}}$ which exactly cancels the overall phase, which from the derivation is given by $\Delta_b = \frac{(K+J)\chi_K^b \chi^c}{2}$, in Eq.25 ($K = 1, J = 0, \chi_K^b = 1$). The full spin correlator is then determined by the matter Fermion correlator. This is exactly the same expression of a local quantum quench as in the pure Kitaev model^{32,33}. Thus, our heavy flux approximation has the correct limit for $J \rightarrow 0$ and can be readily compared with our previous work on the exact solution (notation as in Ref.48)

$$S_{A_0 B_0}^{zz; J, \Gamma=0}(t) = -i \langle 0 | e^{iH^c t} c_{A_0} e^{-(H^c + V_{A_0}^z) t} c_{B_0} | 0 \rangle = -G_{A_0 B_0}^c$$

$$S_{A_0 A_0}^{zz; J, \Gamma=0}(t) = \langle 0 | e^{iH^c t} c_{A_0} e^{-(H^c + V_{A_0}^z) t} c_{A_0} | 0 \rangle = -i G_{A_0 A_0}^c.$$

IV. RESULTS

We concentrate on results obtained for the dynamical structure factor, Eq.2, which is the Fourier transform in space and time of the dynamical spin correlation function defined in Eq.17. Furthermore, to make connection to the inelastic neutron scattering (INS) experiments we also study the intensity of the INS response, $\mathcal{I}(\mathbf{q}, \omega)$, which includes the projectors to the transverse momentum components of the spin direction and the overall decay from the form factor $F(|\mathbf{q}|)$:

$$\mathcal{I}(\mathbf{q}, \omega) = F(q) \sum_{\alpha, \beta} \left(\delta_{\alpha, \beta} - \frac{q^\alpha q^\beta}{q^2} \right) \mathcal{S}^{\alpha\beta}(\mathbf{q}, \omega). \quad (34)$$

A. Robust versus fine-tuned features

Our modified Z_2 MFT and approximations for the spin dynamics recover the exact results of the Kitaev point in the limit $J, \Gamma \rightarrow 0$. Importantly, it can now be extended beyond the integrable point which allows us to discern the fine-tuned features from the robust qualitative behaviour of the correlations representative of the Kitaev QSL phase.

1. Static correlations

First, we discuss the static correlation which can simply be obtained from our main result Eq.25

$$S_{A_0 B_r}^{\alpha\beta} = -\frac{\delta_{\alpha\beta}}{4} G_{A_0 B_r}^c(t=0) G_{A_0 B_r}^\alpha(t=0). \quad (35)$$

Recall, that for the pure Kitaev model correlations are only non-zero for on-site and nearest neighbour correlators. In addition along a z -type bond only S^{zz} correlators were non-zero etc. The main qualitative changes induced by Heisenberg and Γ interaction are summarised as follows, see also Fig.1.

First, correlations between sites of the same sublattice $S_{A_0 A_r}^{\alpha\beta} = \delta_{0,r}$ continue to be only on-site. The reason is the bipartite hopping problem of the c -type matter Majoranas which is unaffected by the extra couplings.

Second, with nonzero but small J or Γ the real space correlations fall off exponentially because they are governed by the flux-propagators deviating from the flat band limit, which was already predicted in Ref.⁴³. Also, with *both* nonzero J, Γ there is a small fourth order algebraic contribution which we neglect here but which has a negligible influence on the total weight of the structure factor in the perturbative regime around the Kitaev point²⁷. Of course, the phase transition out of the ordered state will be driven by divergence of long range correlations, and therefore, the current augmented MFT is only applicable inside the Kitaev QSL phase. It does not capture its breakdown other than indicating a termination of the stability of the phase through the vanishing of the flux gap whence the heavy-flux approximation clearly breaks down.

Third, the strong bond selectivity of the spin correlations is relaxed beyond the Kitaev limit. A non-zero J induces finite $S^{xx,yy}$ correlations along z -bonds (etc.) and a non-zero Γ induces finite $S^{xy,yx}$ correlations along z -bonds (etc.), see the summary in Fig.1. From the quickly decaying static real space spin correlations we can reduce the calculations to a small number of real space correlators, symmetries between real and spin space reduce the number of inequivalent ones further. In addition to the on-site and nearest neighbour correlations we only need to include the three third nearest neighbour correlations for non-zero Γ capturing the leading longer range correlations in space.

2. Dynamical correlations

As has been pointed out previously, the gap in the structure factor of the pure Kitaev model is an artefact of the static fluxes of the integrable Kitaev limit²⁷. Similarly, we find that due to the fact that the suddenly inserted flux from a spin flip can hop away, away from the fine-tuned limit as captured by a finite life-time τ , the gap of the structure factor is filled in. Hence, the overall phase Δ_b of Eq.25 is adjusted self-consistently to

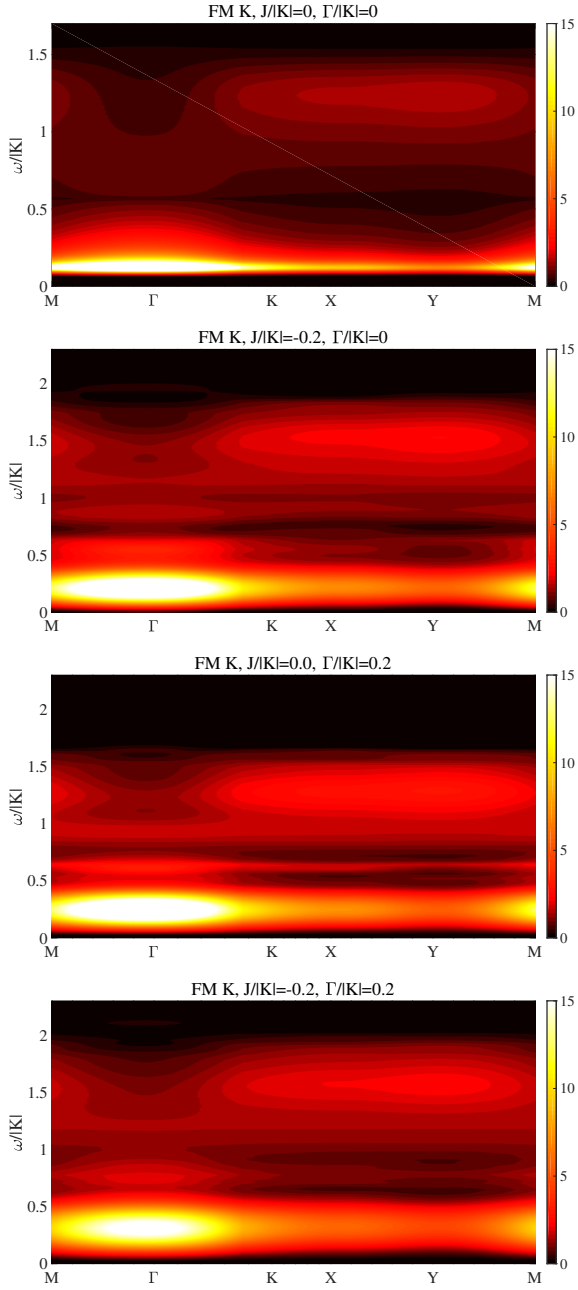


FIG. 5. The dynamical structure factor $\mathcal{S}(\mathbf{q}, \omega)$ is shown along a path through the BZ for different parameters of the Kitaev QSL phase.

obtain the gapless structure factor²⁷ with a low frequency (long time) behaviour determined by the matter propagator $S(\omega) \propto G^c(\omega) \propto \omega$ (governed by the matter fermion DOS linear in ω). Note, only at the Kitaev point do we have precisely $\Delta_b = -C_{A0}^\alpha$ but because of the factorization the overall phase is not simply given by one of the flux gaps.

Second, the new time scale τ has considerable effect on the big low frequency peak dominating the dynamical structure factor of the pure Kitaev model, see Fig. 4.

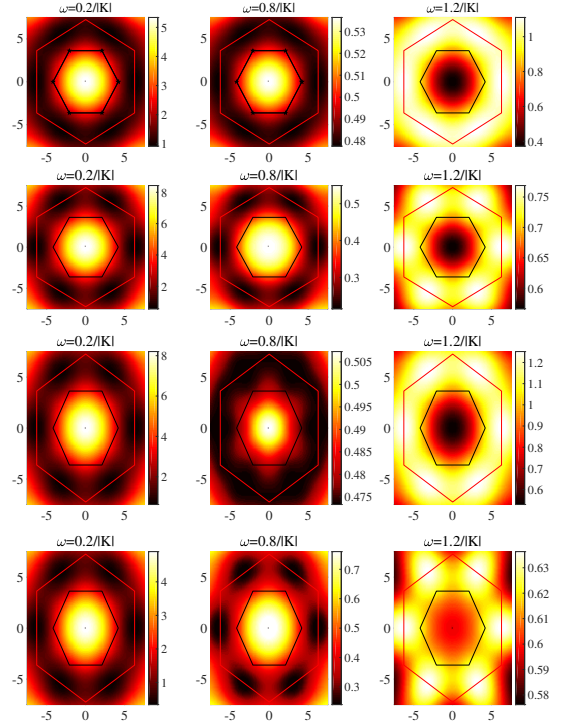


FIG. 6. The dynamical structure factor $\mathcal{S}(\mathbf{q}, \omega)$ is shown over the extended BZ for three different constant frequency cuts. The first (black) and second (red) BZs are indicated. The parameters of each panel are the same as for the corresponding panels in Fig. 5.

This is perhaps the visibly most striking consequence of integrability breaking – more spectral weight is transferred to higher energies asymmetrically and anisotropically in presence of Γ . Moreover, the sharp peak at low energies is broadened in an asymmetric fashion and the magnetic bandwidth is reduced/increased.

Third, the momentum dependence is changed because the strong bond selectivity is relaxed, e.g. a nonzero J induces $S^{xx/yy}$ correlations along a z -type bond, etc. In Figs. 5 and 6 four representative regimes of the structure factor are shown. Note, however that the gross qualitative features of the FM Kitaev QSL – a low energy peak in intensity at the Γ -point and a corresponding minimum of intensity for high energies – is robust. Moreover, the overall magnetic bandwidth corresponding to the matter Majorana Fermions and the minimum of intensity at the energy scale of the van Hove singularity of the Majorana fermions is another feature in common with the pure Kitaev model^{32,33}. The corresponding MFT band structures of the matter- and flux-Majorana Fermions are presented in Fig. 2.

Finally, because of the dynamical nature of the fluxes, the intensity, which was mainly concentrated in a narrow low energy peak for the pure Kitaev point, is redistributed to higher energies.

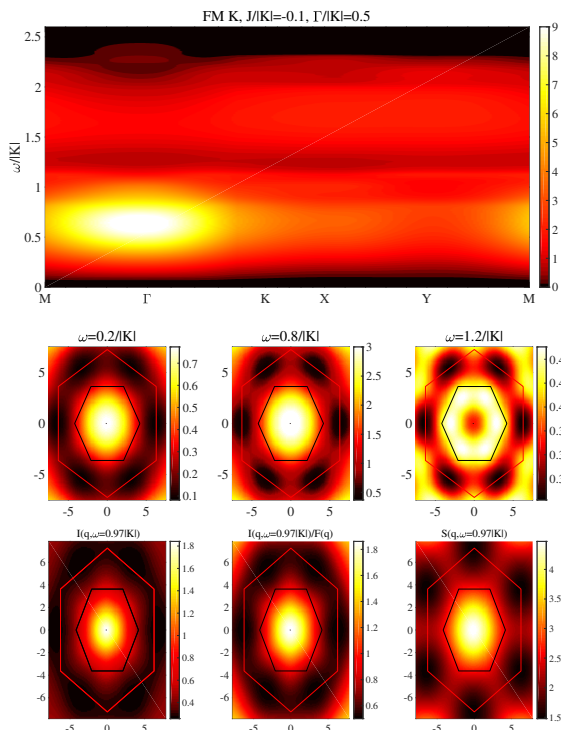


FIG. 7. Dynamical spin correlation for the FM Kitaev QSL with the best-fit model parameters for α -RuCl₃ from Winter *et al.*³¹ $J = -0.1$, $\Gamma = 0.5$. Path through the BZ (upper panel) of the structure factor $\mathcal{S}(\mathbf{q}, \omega)$ without the spin-momentum projectors (no form factor decay) and constant frequency cuts (middle) including the projectors (no form factor decay). The lower panel shows the effect of the projectors for a constant frequency cut at $\omega = 0.97|K|$. The left panel shows the full INS scattering intensity $\mathcal{I}(\mathbf{q}, \omega)$, Eq.34, the middle panel without the decay $F(q)$ and the right panel the bare structure factor without the momentum projectors. It shows that the combination of the projector and the off-diagonal spin correlations induced by the Γ term are one possible source for the star-like pattern observed in α -RuCl₃.

B. Connection to α -RuCl₃

Our work is partially motivated by the recent INS results on the honeycomb Kitaev candidate material α -RuCl₃ which shows unusual broad scattering continua reminiscent of the ones calculated for the pure Kitaev model^{34,35,38}. However, agreement is only partial, with discrepancies concerning the overall intensity distribution as a function of frequency, as well as details of the momentum dependence. Note also that the low frequency response of α -RuCl₃ at low temperatures should be related to the weak residual long range magnetic ordering.

Contributing to this ongoing discussion we show the structure factor and INS intensity for the recently proposed best fit parameters³¹ for α -RuCl₃ in Fig. 7. Note that despite the fact that the true ground state for these values for the exchange constants has weak long range magnetic order, our parton MFT continues to provide a

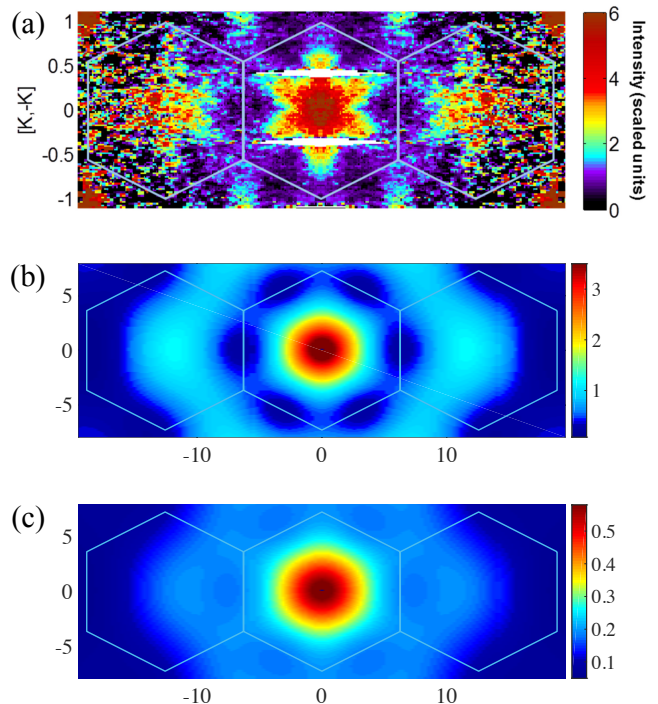


FIG. 8. Comparison of the INS intensity for α -RuCl₃ in panel (a), figure adapted from Ref.35, with that calculated for the best-fit model parameters for α -RuCl₃ from Ref. Winter *et al.*³¹ $J = -0.1$, $\Gamma = 0.5$ in panel (b) and the exact solution of the pure Kitaev model panel (c). For concreteness we chose an energy $\omega/|K| = 0.64$.

(globally unstable) QSL solution. This is evidenced in that, for $\Gamma/|K| = 0.5$ the flux gap goes to zero, see Fig.2 right panel. Therefore, strictly speaking this corresponds to a regime where our approximate treatment is uncontrolled. It is thus all the more striking that our present approach is able to give the following main qualitative changes raising the hope that in the actual material, the high energy spectral weight may remain unaffected by the low energy magnetic ordering and is determined by the proximate QSL physics.

In the frequency domain, the central feature is the dominant peak at low frequencies above the flux gap. This is much narrower in the integrable case than for our theory using the best-fit parameters, which is indeed closer to what is found in experiment.

In wavevector space, Fig.8, the central peak for the integrable model is quite broad, covering the full Brillouin zone in that the minimum at the zone edge is relatively shallow (lower panel). This reflects the very short-range correlations of the integrable model. By contrast, for the best-fit model (middle panel), the corresponding minimum is considerably more pronounced, as it is in experiment (upper panel).

Also in Fig.8, a six-fold star pattern is very visible in the experimental data, which is almost entirely absent in the integrable case. A six-fold angular modulation is still rather weak in the best-fit model, but it is starting to be

visible there, e.g. in the form of higher scattering intensity at the K points (Brioullin zone corners) compared to the M points (midpoints of Brioullin zone edges). This can be traced back to a combination of the momentum-spin projectors relating the structure factor to the INS intensity, see Eq.34 and the spin off-diagonal terms induced by the Γ term. We show a comparison of the scattering in the entire BZ with and without the momentum projectors in the lower panel of Fig.7, where the six-fold structure is considerably stronger.

Overall, it is encouraging that the best-fit parameters used for our augmented theory hence provide qualitative changes of the exact solution heading in the correct direction with respect to experiment on α -RuCl₃, but they still do not provide quantitative agreement. Whether this is due to the fact that the ‘perturbations’ in the experimental system there are simply too large, or that the best-fit parameters do not present the final answer themselves, or both, is something we are at present unable to settle.

V. DISCUSSION AND OUTLOOK

Beyond the immediate desire to account for experimental results in Kitaev candidate compounds, we would finally like to address how this work fits into the broader picture of studies of quantum spin liquids and fractionalised correlated phases more generally.

It has been known for a long time that the ground state of the Kitaev honeycomb model can exactly be captured by a parton-based mean-field theory. What was possibly less appreciated is that this does not extend to excited states; and by dint of this, to the dynamics even at zero temperature. Our theory plugs this gap, and hence embeds the exactly soluble Kitaev model in the lore of parton theories, from the perspective of which a dynamical analysis like the one possible here is non-trivial in itself.

This exactly soluble augmented parton theory thus provides a controlled starting point for the inclusion of integrability-breaking terms. We choose to include the popular Heisenberg and Γ terms, as these are believed to play a role in an experimentally relevant setting, as well as providing different flavours of integrability-breaking, both each in isolation, and in combination.

Our treatment focuses on the leading effect of these perturbations on the ‘bulk’ of the response, as loosely defined by spectral weight. Our treatment thus omits some terms which are perturbatively small (higher order) in the perturbations, such as a term of order $J_H^2 \Gamma^2$, which however is dominant in the long-distance limit, where it engenders an algebraically small tail to the correlations with a tiny prefactor. By contrast, our theory does account for a lower-order shift of the bulk of the spectral weight. In this sense, our analysis should be seen as a complement to that of Ref.27.

Of course, when these high-order perturbations cease to be small, our theory ceases to be justified. It will

thus, in its present simple form, systematically fail to account with any degree of accuracy for the termination of the spin liquid phase, which would generically go along with a breakdown of the fractionalisation in the form of a re-binding of the partons, and an increase (and eventually divergence) of the weight in the long-range part of the correlations. On top of this, our heavy flux approximation is not systematic, and there is presumably still considerable scope for alternative, optimised schemes beyond this first pass. Our derivation and first analysis of this augmented MFT immediately points in a number of directions for future work.

A first task is to extend the reach of the present analysis by targeting a larger class of experimental observables and computing the relevant responses of other experimentally relevant probes, such as ESR^{49,50}, Raman scattering^{37,51–54} or resonant inelastic X-ray scattering (RIXS)⁵⁵.

Perhaps the most obvious new direction is the inclusion of other perturbations of experimental interest, most saliently a magnetic field^{36,56,57}. This would allow to contrast the effect of the removal of time-reversal symmetry with and without retention of integrability.

Next on the wishlist would be the extension to other regimes; a finite-temperature treatment⁵⁸ again being motivated by the experimentally suggested existence of a proximate spin liquid whose ‘parasitic’ magnetic order melts above a finite Néel temperature, presenting a finite-temperature magnetically disordered target regime³⁴.

On the technical/conceptual front, a more comprehensive inclusion of the spinon-vison (Majorana-flux) coupling is clearly desirable, as this would extend the theory towards the inclusion of instabilities of the spin liquid phase. Such an analysis would also be of interest to other cases of popular spin liquids, such as the perennial problem of the kagome lattice quantum antiferromagnet⁵⁹.

Considerably more ambitious would be the extension of these ideas to other types of many-body states. A theory of a fractionalised magnetically ordered phase would be a worthy goal indeed in this framework.

Overall, we feel that our novel augmented Z_2 parton MFT strikes an attractive balance between solubility, controllability, and genericity. Hence, we believe it will be of more general interest for the study of topological QSLs beyond the example presented here of the paradigmatic Kitaev QSL phase.

ACKNOWLEDGEMENTS

We acknowledge helpful discussions with Yong Baek Kim, Frank Pollmann, Achim Rosch, Adam Smith and Roser Valenti. We are also very grateful to Ganapathy Baskaran, John Chalker, Matthias Gohlke, Dima Kovrizhin, Yong Baek Kim, Saptarshi Mandal, Frank Pollmann, Robert Schaffer, Krishnendu Sengupta, R. Shankar and Ruben Verresen for collaboration on related subjects. SB acknowledges MPG for funding through the

partner group at ICTS, MIPPKS for hospitality and support of the DST (India) project ECR/2017/000504. This work was in part supported by the Deutsche Forschungsgemeinschaft under grant SFB 1143. Statement of com-

pliance with EPSRC policy framework on research data: All data accompanying this publication are directly available within the publication.

-
- ¹ B. Lake, D. A. Tennant, J.-S. Caux, T. Barthel, U. Schollwöck, S. E. Nagler, and C. D. Frost, *Phys. Rev. Lett.* **111**, 137205 (2013).
- ² P. W. Anderson, *science* **235**, 1196 (1987).
- ³ X.-G. Wen, *Quantum field theory of many-body systems: from the origin of sound to an origin of light and electrons* (Oxford University Press on Demand, 2004).
- ⁴ G. Misguich, C. Lhuillier, and H. Diep, “Frustrated spin systems,” (2005).
- ⁵ P. A. Lee, *Science* **321**, 1306 (2008).
- ⁶ L. Balents, *Nature* **464**, 199 (2010).
- ⁷ A. Kitaev, *Annals of Physics* **321**, 2 (2006), january Special Issue.
- ⁸ G. Baskaran and P. W. Anderson, *Phys. Rev. B* **37**, 580 (1988).
- ⁹ G. Baskaran, Z. Zou, and P. Anderson, *Solid state communications* **63**, 973 (1987).
- ¹⁰ I. Affleck and J. B. Marston, *Phys. Rev. B* **37**, 3774 (1988).
- ¹¹ G. Kotliar and J. Liu, *Phys. Rev. B* **38**, 5142 (1988).
- ¹² P. A. Lee, N. Nagaosa, and X.-G. Wen, *Rev. Mod. Phys.* **78**, 17 (2006).
- ¹³ X.-G. Wen, *Phys. Rev. B* **65**, 165113 (2002).
- ¹⁴ N. Read and S. Sachdev, *Phys. Rev. Lett.* **62**, 1694 (1989).
- ¹⁵ N. Read and S. Sachdev, *Phys. Rev. B* **42**, 4568 (1990).
- ¹⁶ N. Read and S. Sachdev, *Phys. Rev. Lett.* **66**, 1773 (1991).
- ¹⁷ D. P. Arovas and A. Auerbach, *Physical Review B* **38**, 316 (1988).
- ¹⁸ A. Auerbach and D. P. Arovas, *Physical review letters* **61**, 617 (1988).
- ¹⁹ X. Chen and M. Hermele, *Phys. Rev. B* **94**, 195120 (2016).
- ²⁰ T. Dodds, S. Bhattacharjee, and Y. B. Kim, *Phys. Rev. B* **88**, 224413 (2013).
- ²¹ M. J. Lawler, H.-Y. Kee, Y. B. Kim, and A. Vishwanath, *Phys. Rev. Lett.* **100**, 227201 (2008).
- ²² M. Punk, D. Chowdhury, and S. Sachdev, *Nature Physics* **10**, 289 (2014).
- ²³ R. Schaffer, S. Bhattacharjee, and Y. B. Kim, *Phys. Rev. B* **88**, 174405 (2013).
- ²⁴ F. J. Burnell and C. Nayak, *Phys. Rev. B* **84**, 125125 (2011).
- ²⁵ Y.-Z. You, I. Kimchi, and A. Vishwanath, *Phys. Rev. B* **86**, 085145 (2012).
- ²⁶ R. Schaffer, S. Bhattacharjee, and Y. B. Kim, *Phys. Rev. B* **86**, 224417 (2012).
- ²⁷ X.-Y. Song, Y.-Z. You, and L. Balents, *Phys. Rev. Lett.* **117**, 037209 (2016).
- ²⁸ J. c. v. Chaloupka, G. Jackeli, and G. Khaliullin, *Phys. Rev. Lett.* **105**, 027204 (2010).
- ²⁹ D. Gotfryd, J. Rusnačko, K. Wohlfeld, G. Jackeli, J. c. v. Chaloupka, and A. M. Oleś, *Phys. Rev. B* **95**, 024426 (2017).
- ³⁰ M. Gohlke, R. Verresen, R. Moessner, and F. Pollmann, *Phys. Rev. Lett.* **119**, 157203 (2017).
- ³¹ S. M. Winter, K. Riedl, A. Honecker, and R. Valenti, *arXiv:1702.08466* (2017).
- ³² J. Knolle, D. L. Kovrizhin, J. T. Chalker, and R. Moessner, *Phys. Rev. Lett.* **112**, 207203 (2014).
- ³³ J. Knolle, D. L. Kovrizhin, J. T. Chalker, and R. Moessner, *Phys. Rev. B* **92**, 115127 (2015).
- ³⁴ A. Banerjee, C. Bridges, J.-Q. Yan, A. Aczel, L. Li, M. Stone, G. Granroth, M. Lumsden, Y. Yiu, J. Knolle, *et al.*, *Nature materials* **15**, 733 (2016).
- ³⁵ A. Banerjee, J. Yan, J. Knolle, C. A. Bridges, M. B. Stone, M. D. Lumsden, D. G. Mandrus, D. A. Tennant, R. Moessner, and S. E. Nagler, *Science* **356**, 1055 (2017).
- ³⁶ A. Banerjee, P. Lampen-Kelley, J. Knolle, C. Balz, A. Aczel, B. Winn, Y. Liu, D. Pajerowski, J.-Q. Yan, C. Bridges, *et al.*, *arXiv preprint arXiv:1706.07003* (2017).
- ³⁷ J. Nasu, J. Knolle, D. L. Kovrizhin, Y. Motome, and R. Moessner, *Nature Physics* **12**, 912 (2016).
- ³⁸ S.-H. Do, S.-Y. Park, J. Yoshitake, J. Nasu, Y. Motome, Y. S. Kwon, D. Adroja, D. Voneshen, K. Kim, T.-H. Jang, *et al.*, *Nature Physics* (2017).
- ³⁹ M. Hermanns, I. Kimchi, and J. Knolle, *Annual Review of Condensed Matter Physics* **9**, null (2018), *arXiv:1705.01740*.
- ⁴⁰ S. M. Winter, A. A. Tsirlin, M. Daghofer, J. van den Brink, Y. Singh, P. Gegenwart, and R. Valenti, *Journal of Physics: Condensed Matter* **29**, 493002 (2017).
- ⁴¹ A. Smith, J. Knolle, D. L. Kovrizhin, J. T. Chalker, and R. Moessner, *Phys. Rev. B* **92**, 180408 (2015).
- ⁴² A. Smith, J. Knolle, D. L. Kovrizhin, J. T. Chalker, and R. Moessner, *Phys. Rev. B* **93**, 235146 (2016).
- ⁴³ S. Mandal, S. Bhattacharjee, K. Sengupta, R. Shankar, and G. Baskaran, *Phys. Rev. B* **84**, 155121 (2011).
- ⁴⁴ G. Baskaran, S. Mandal, and R. Shankar, *Phys. Rev. Lett.* **98**, 247201 (2007).
- ⁴⁵ H. Yao and S. A. Kivelson, *Phys. Rev. Lett.* **99**, 247203 (2007).
- ⁴⁶ F. L. Pedrocchi, S. Chesi, and D. Loss, *Phys. Rev. B* **84**, 165414 (2011).
- ⁴⁷ F. Zschocke and M. Vojta, *Phys. Rev. B* **92**, 014403 (2015).
- ⁴⁸ J. Knolle, *Dynamics of a Quantum Spin Liquid* (Springer, 2016).
- ⁴⁹ Z. Wang, S. Reschke, D. Hüvonen, S.-H. Do, K.-Y. Choi, M. Gensch, U. Nagel, T. Röm, and A. Loidl, *Phys. Rev. Lett.* **119**, 227202 (2017).
- ⁵⁰ A. Little, L. Wu, P. Lampen-Kelley, A. Banerjee, S. Patankar, D. Rees, C. A. Bridges, J.-Q. Yan, D. Mandrus, S. E. Nagler, and J. Orenstein, *Phys. Rev. Lett.* **119**, 227201 (2017).
- ⁵¹ L. J. Sandilands, Y. Tian, K. W. Plumb, Y.-J. Kim, and K. S. Burch, *Phys. Rev. Lett.* **114**, 147201 (2015).
- ⁵² A. Glamazda, P. Lemmens, S.-H. Do, Y. S. Kwon, and K.-Y. Choi, *Phys. Rev. B* **95**, 174429 (2017).
- ⁵³ B. Perreault, J. Knolle, N. B. Perkins, and F. J. Burnell, *Phys. Rev. B* **92**, 094439 (2015).
- ⁵⁴ B. Perreault, J. Knolle, N. B. Perkins, and F. J. Burnell, *Phys. Rev. B* **94**, 104427 (2016).

- ⁵⁵ G. B. Halász, B. Perreault, and N. B. Perkins, Phys. Rev. Lett. **119**, 097202 (2017).
- ⁵⁶ S.-H. Baek, S.-H. Do, K.-Y. Choi, Y. S. Kwon, A. U. B. Wolter, S. Nishimoto, J. van den Brink, and B. Büchner, Phys. Rev. Lett. **119**, 037201 (2017).
- ⁵⁷ J. A. Sears, Y. Zhao, Z. Xu, J. W. Lynn, and Y.-J. Kim, Phys. Rev. B **95**, 180411 (2017).
- ⁵⁸ J. Nasu, M. Udagawa, and Y. Motome, Phys. Rev. Lett. **113**, 197205 (2014).
- ⁵⁹ M. R. Norman, Rev. Mod. Phys. **88**, 041002 (2016).

Appendix A: Mean-field solution and self-consistency equations

1. MFT solutions c -type matter Majorana Fermions

In the vicinity of the pure Kitaev QSL the ground state remains in the flux-free sector with all $u_{ij} = ib_i^\alpha b_j^\alpha = 1 = \sigma_{ij}^\alpha$. Here we show details of the diagonalization of the MF Hamiltonian Eq.16 in the ground state flux sector. Note that the additional interactions only change the overall bandwidth of the c -type Hamiltonian but leave the dispersion and wave functions unchanged. First, we concentrate on the matter Majorana fermions. Introducing complex fermions with a new notation with the two sublattices labeled by A/B

$$c_{A\mathbf{r}} = (f_{\mathbf{r}} + f_{\mathbf{r}}^\dagger) \quad \text{and} \quad c_{B\mathbf{r}} = i(f_{\mathbf{r}} - f_{\mathbf{r}}^\dagger) \quad (\text{A1})$$

and their Fourier transformation $f_{\mathbf{r}} = \frac{1}{\sqrt{N_b}} \sum_{\mathbf{q}} e^{-i\mathbf{q}\mathbf{r}} f_{\mathbf{q}}$ the Hamiltonian can be written in a standard Bogoliubov-de-Gennes form

$$H^c = \sum_{\mathbf{q}} [f_{\mathbf{q}}^\dagger \quad f_{-\mathbf{q}}] \begin{bmatrix} \xi_{\mathbf{q}} & -\Delta_{\mathbf{q}} \\ -\Delta_{\mathbf{q}}^* & -\xi_{\mathbf{q}} \end{bmatrix} \begin{bmatrix} f_{\mathbf{q}} \\ f_{-\mathbf{q}}^\dagger \end{bmatrix} \quad (\text{A2})$$

with the definitions

$$S(\mathbf{q}) = \left[\frac{K+J}{4} \chi_K^b + \frac{J}{2} \chi_J^b + \frac{\Gamma}{2} \chi_\Gamma^b \right] (1 + e^{i\mathbf{q}\mathbf{n}_x} + e^{i\mathbf{q}\mathbf{n}_y}) \quad (\text{A3})$$

$\xi_{\mathbf{q}} = \text{Re}S(\mathbf{q})$ and $\Delta_{\mathbf{q}} = -i\text{Im}S(\mathbf{q})$. The lattice vectors are $\mathbf{n}_{x/y} = (\pm\frac{1}{2}, \frac{\sqrt{3}}{2})$ and the vector connecting the sublattices is $\delta = (0, -\frac{1}{\sqrt{3}})$, see Fig.1 (a).

A standard Bogoliubov rotation

$$\begin{bmatrix} f_{\mathbf{q}} \\ f_{-\mathbf{q}}^\dagger \end{bmatrix} = \begin{bmatrix} \cos\theta_{\mathbf{q}} & i\sin\theta_{\mathbf{q}} \\ i\sin\theta_{\mathbf{q}} & \cos\theta_{\mathbf{q}} \end{bmatrix} \begin{bmatrix} a_{\mathbf{q}} \\ a_{-\mathbf{q}}^\dagger \end{bmatrix} \quad (\text{A4})$$

with $\tan 2\theta_{\mathbf{q}} = -\frac{\text{Im}S(\mathbf{q})}{\text{Re}S(\mathbf{q})}$ diagonalizes the system

$$H^c = \sum_{\mathbf{q}} 2|S(\mathbf{q})| \left[a_{\mathbf{q}}^\dagger a_{\mathbf{q}} - \frac{1}{2} \right] \quad (\text{A5})$$

such that the Heisenberg equation of motion directly gives the time dependence of the operators

$$a_{\mathbf{q}}(t) = a_{\mathbf{q}} e^{-it2|S(\mathbf{q})|}. \quad (\text{A6})$$

2. MFT solutions b -type flux Majorana Fermions

First, for $\Gamma = 0$ the Hamiltonian of the different b -type Majoranas decouples and we can introduce three different complex fermions with $\alpha = x, y, z$ [and define $\mathbf{n}_z = (0, 0)$]

$$b_{A\mathbf{r}}^\alpha = (f_{\mathbf{r}}^\alpha + f_{\mathbf{r}}^{\alpha\dagger}) \quad \text{and} \quad b_{B\mathbf{r}+\mathbf{n}_\alpha}^\alpha = i(f_{\mathbf{r}}^\alpha - f_{\mathbf{r}}^{\alpha\dagger}) \quad (\text{A7})$$

and their Fourier transformation $f_{\mathbf{r}}^\alpha = \frac{1}{\sqrt{N_B}} \sum_{\mathbf{q}} e^{-i\mathbf{q}\mathbf{r}} f_{\mathbf{q}}^\alpha$. The b -type MFT Hamiltonian can be written in a standard Bogoliubov-de-Gennes form

$$H^b = \sum_{\alpha} \sum_{\mathbf{q}} [f_{\mathbf{q}}^{\alpha\dagger} \quad f_{-\mathbf{q}}^\alpha] \begin{bmatrix} \xi_{\mathbf{q}}^\alpha & -\Delta_{\mathbf{q}}^\alpha \\ -\Delta_{\mathbf{q}}^{\alpha*} & -\xi_{\mathbf{q}}^\alpha \end{bmatrix} \begin{bmatrix} f_{\mathbf{q}}^\alpha \\ f_{-\mathbf{q}}^{\alpha\dagger} \end{bmatrix} \quad (\text{A8})$$

with the definitions $\xi_{\mathbf{q}}^\alpha = \frac{K\chi^c}{4} + \frac{J\chi^c}{4} \text{Re} \sum_{\beta \neq \alpha} e^{-i\mathbf{q}(\mathbf{n}_\beta - \mathbf{n}_\alpha)}$ and $\Delta_{\mathbf{q}}^\alpha = i\frac{J\chi^c}{4} \text{Im} \sum_{\beta \neq \alpha} e^{-i\mathbf{q}(\mathbf{n}_\beta - \mathbf{n}_\alpha)}$.

As before, a standard Bogoliubov rotation

$$\begin{bmatrix} f_{\mathbf{q}}^\alpha \\ f_{-\mathbf{q}}^{\alpha\dagger} \end{bmatrix} = \begin{bmatrix} \cos\theta_{\mathbf{q}}^\alpha & i\sin\theta_{\mathbf{q}}^\alpha \\ i\sin\theta_{\mathbf{q}}^\alpha & \cos\theta_{\mathbf{q}}^\alpha \end{bmatrix} \begin{bmatrix} a_{\mathbf{q}}^\alpha \\ a_{-\mathbf{q}}^{\alpha\dagger} \end{bmatrix} \quad (\text{A9})$$

with $\tan 2\theta_{\mathbf{q}}^\alpha = -\frac{i\Delta_{\mathbf{q}}^\alpha}{\xi_{\mathbf{q}}^\alpha}$ diagonalizes the system

$$H^b = \sum_{\mathbf{q}} 2|S^\alpha(\mathbf{q})| \left[a_{\mathbf{q}}^{\alpha\dagger} a_{\mathbf{q}}^\alpha - \frac{1}{2} \right]. \quad (\text{A10})$$

such that the dispersion $|S^\alpha(\mathbf{q})| = \sqrt{|\xi_{\mathbf{q}}^\alpha|^2 + |\Delta_{\mathbf{q}}^\alpha|^2}$ determines the time dependence similar to Eq.A6.

Second, for nonzero Γ the different sectors $\alpha = x, y, z$ of the flux-type Majoranas are all coupled. We use the standard Fourier transform $b_{A\mathbf{r}}^\alpha = \frac{1}{\sqrt{N_b}} \sum_{\mathbf{q}} e^{-i\mathbf{q}\mathbf{r}} b_{A\mathbf{q}}^\alpha$ and because Majoranas are their own adjoints we get $b_{A\mathbf{q}}^{\alpha\dagger} = b_{A-\mathbf{q}}^\alpha$. Then we write the Hamiltonian as

$$H^b = \sum_{\mathbf{q}} [b_{A\mathbf{q}}^x \quad b_{A\mathbf{q}}^y \quad b_{A\mathbf{q}}^z] i\hat{M}_{\mathbf{q}} \begin{bmatrix} b_{B-\mathbf{q}}^x \\ b_{B-\mathbf{q}}^y \\ b_{B-\mathbf{q}}^z \end{bmatrix} = \sum_{\mathbf{q}, j=1,2,3} i\epsilon_{\mathbf{q}}^j \phi_{j\mathbf{q}}^A \phi_{j-\mathbf{q}}^B \quad \text{with} \quad (\text{A11})$$

$$\hat{M}_{\mathbf{q}} = -\frac{\chi^c}{4} \begin{bmatrix} (J+K)e^{i\mathbf{q}\mathbf{n}_x} + J(e^{i\mathbf{q}\mathbf{n}_y} + 1) & \Gamma & \Gamma e^{i\mathbf{q}\mathbf{n}_y} \\ \Gamma & (J+K)e^{i\mathbf{q}\mathbf{n}_y} + J(e^{i\mathbf{q}\mathbf{n}_x} + 1) & \Gamma e^{i\mathbf{q}\mathbf{n}_x} \\ \Gamma e^{i\mathbf{q}\mathbf{n}_y} & \Gamma e^{i\mathbf{q}\mathbf{n}_x} & (J+K) + J(e^{i\mathbf{q}\mathbf{n}_x} + e^{i\mathbf{q}\mathbf{n}_y}) \end{bmatrix} \quad (\text{A12})$$

and the singular value decomposition $\hat{M}_{\mathbf{q}} = \hat{U}_{\mathbf{q}} \hat{\Lambda}_{\mathbf{q}} \hat{V}_{\mathbf{q}}^\dagger$ with the positive real diagonal matrix $\text{diag} \hat{\Lambda}_{\mathbf{q}} = [\epsilon_{\mathbf{q}}^1, \epsilon_{\mathbf{q}}^2, \epsilon_{\mathbf{q}}^3]$ and $b_{A\mathbf{q}}^\alpha = \sum_j U_{j\mathbf{q}}^\alpha \phi_{j\mathbf{q}}^A$ and $b_{B-\mathbf{q}}^\alpha = \sum_j V_{j\mathbf{q}}^\alpha \phi_{j-\mathbf{q}}^B$ with $U_{j\mathbf{q}}^\alpha$ the matrix elements of $\hat{U}_{\mathbf{q}}^\dagger$ (α labels the columns) and $V_{j\mathbf{q}}^\alpha$ the matrix elements of $\hat{V}_{\mathbf{q}}$ (α labels the rows). Note, from $\hat{M}_{-\mathbf{q}} = \hat{M}_{\mathbf{q}}^*$ we get $\hat{\Lambda}_{-\mathbf{q}} = \hat{\Lambda}_{\mathbf{q}}$ and for the unitary matrices $\hat{U}_{-\mathbf{q}} = U_{\mathbf{q}}^*$ and $\hat{V}_{-\mathbf{q}} = V_{\mathbf{q}}^*$.

Finally, with the use of standard complex fermions

$$\phi_{j\mathbf{q}}^A = f_{j\mathbf{q}}^b + f_{j-\mathbf{q}}^{b\dagger} \quad (\text{A13})$$

$$\phi_{j\mathbf{q}}^B = -i \left\{ f_{j\mathbf{q}}^b - f_{j-\mathbf{q}}^{b\dagger} \right\} \quad (\text{A14})$$

$$(\text{A15})$$

we obtain

$$H^b = \sum_{\mathbf{q}, j=1,2,3} 2\epsilon_{\mathbf{q}}^j \left\{ f_{j\mathbf{q}}^{b\dagger} f_{j\mathbf{q}}^b - \frac{1}{2} \right\}. \quad (\text{A16})$$

such that the dispersions $2\epsilon_{\mathbf{q}}^j$ determines the time dependence similar to Eq.A6.

3. Self-consistency equations

We have four different mean-field parameters each of which is determined by its own self-consistency equation. First, the one from the matter fermions

$$\chi^c = i \langle c_{A0} c_{B0} \rangle = 2 \sum_{\mathbf{q}} \cos^2 \theta_{\mathbf{q}} - 1 = 0.5249 \quad (\text{A17})$$

which is independent of the values K, J, Γ and $\chi_{J/K/\Gamma}^b$. There are three equations for the flux-fermions.

$$\chi_K^b = i \langle b_{A0}^z b_{B0}^z \rangle = - \sum_{\mathbf{q}, j} U_{j\mathbf{q}}^z V_{j\mathbf{q}}^z \quad (\text{A18})$$

$$\chi_J^b = i \langle b_{A0}^x b_{B0}^x \rangle = - \sum_{\mathbf{q}, j} U_{j\mathbf{q}}^x V_{j\mathbf{q}}^x \quad (\text{A19})$$

$$\chi_\Gamma^b = i \langle b_{A0}^x b_{B0}^y \rangle = - \sum_{\mathbf{q}, j} U_{j\mathbf{q}}^x V_{j\mathbf{q}}^y \quad (\text{A20})$$

The evolution of the the order parameters as a function of the different exchange couplings is plotted in Fig.9. The MFT dispersions of the different types of excitations are shown in Fig.2 for representative parameter values.

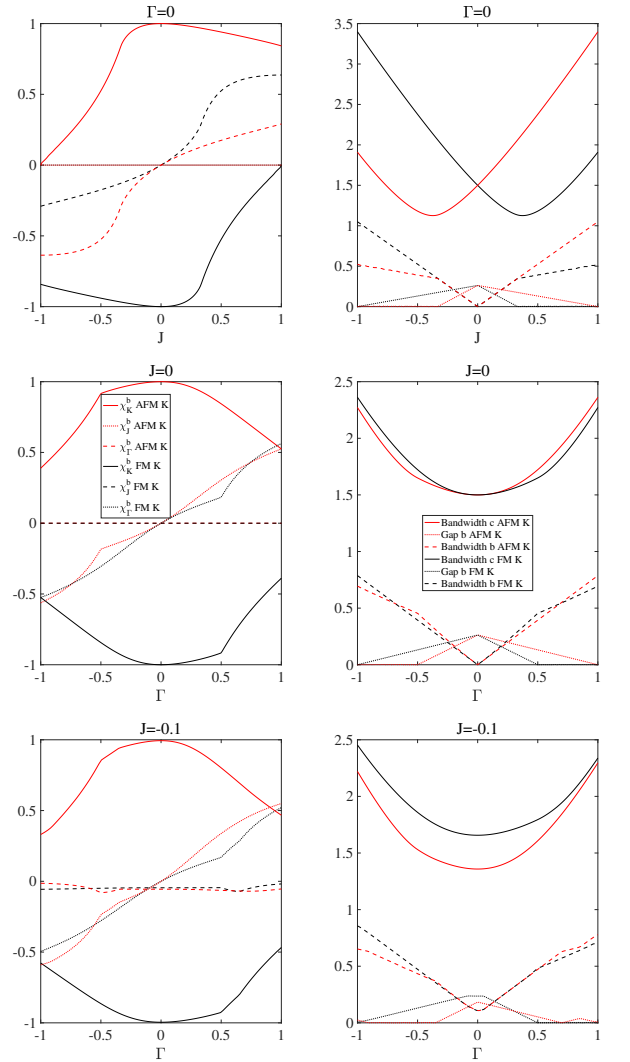


FIG. 9. Evolution of the order parameters as a function of the exchange couplings (left panels); e.g. varying J for $\Gamma = 0$ (upper panels), varying Γ for $J = 0$ (middle panels), and varying Γ for FM $J = -0.1$ (lower panels). The right panel shows the corresponding change in the bandwidth for the c -type and b -type Majorana fermions and the evolution of the gap of the b 's, see the inset of the middle panels for the legends.